Abnormal hole mobility of biaxial strained Si

M. H. Liao
Department of Electrical Engineering and Graduate Institute of Electro-Optical Engineering, National Taiwan University, Taipei, Taiwan, Republic of China

S. T. Chang
Department of Electrical Engineering, National Chung Hsing University, Taichung, Taiwan, Republic of China

M. H. Lee and S. Maikap
Electronics Research & Service Organization, Industrial Technology Research Institute, Hsinchu, Taiwan, Republic of China

C. W. Liu[a)]
Department of Electrical Engineering, Graduate Institute of Electro-Optical Engineering, and Graduate Institute of Electronic Engineering, National Taiwan University, Taipei, Taiwan, Republic of China

(Received 24 March 2005; accepted 1 August 2005; published online 20 September 2005)

The strain effect on the hole mobility is investigated by bulk Si field-effect transistor, substrate-strained Si devices, and these devices under biaxial tensile mechanical strain. The hole mobility along ⟨110⟩ direction on (001) Si substrate degrades at small biaxial tensile strain ($<\sim 0.3\%$) but enhances at the biaxial tensile strain larger than ~0.3%. This abnormal behavior can be understood in terms of the effective hole conductive mass which is the population average of heavy-hole and light-hole masses. The effective mass is more heavy-hole-like at small strain, since the heavy-hole band has a larger density of state than light-hole band. As the biaxial tensile strain increases, the hole population in the light-hole band increases due to the upshift and crossover of the light-hole band above the heavy-hole band. Therefore, the effective mass with larger biaxial tensile strain decreases significantly due to the small mass of light hole. The effective hole mass, which increases at small strain, then decreases at large strain, is responsible to the abnormal hole mobility behavior. © *2005 American Institute of Physics*. [DOI: 10.1063/1.2041839]

Substrate-strained Si as a mobility-enhanced technology has received considerable attention in the last decade and becomes practical for industry applications.[1–5] The mechanism of electron mobility enhancement in substrate-strained Si *n*-channel metal-oxide-semiconductor field-effect transistors (NMOSFETs) is well understood in terms of the splitting of six-fold degenerate Δ valleys, which causes the increase of electron population in the two valleys with lighter conductive mass along the channel and the suppression of the intervalley phonon scattering. On the other hand, the warpage nature of valence band results in the complicated behavior of hole mobility. The previous calculation[5] of hole mobility shows a monotonic increase under biaxial tensile strain at high field. However, in our study, the small mechanical biaxial strain (0.037%) on bulk *p*-channel MOSFET (PMOSFET) causes the degradation of hole mobility at intermediate field, and similar results are also reported by other groups.[6,7] No theoretical calculations are given in the previous work. We, therefore, give the theoretic calculation and compared with the experimental data. The abnormal behavior can be attributed to the initial increase of the effective hole conductive mass at small strain.

The experimental setup to apply the mechanical biaxial tensile strain (~0.037%) is similar to Ref. 8. The undoped strained-Si layers (20 nm thick) were grown by ultrahigh-vacuum chemical-vapor deposition on the relaxed $Si_{0.8}Ge_{0.2}$ (1 μm thick) virtual substrate at 600 °C using SiH_4 and GeH_4 precursors. The relaxed $Si_{0.8}Ge_{0.2}$ layers were grown on the graded $Si_{1-x}Ge_x$ layers (1 μm thick) using the Ge content from 0% to 20%. The strain in the substrate-strained Si device is observed to be ~0.64% by Raman spectroscopy measurement. The bulk Si and substrate-strained Si PMOSFETs were fabricated by a conventional process.[9] The source/drain doping activation condition is 900 °C for 25 min. To avoid the strain relaxation in the substrate-strained Si devices, the gate oxide [tetraethylorthosilicate (TEOS)] with a thickness of ~30 nm was deposited at 700° C. The channel-doping concentration is estimated to be $\sim 1\times 10^{16}$ cm^{-3} for both bulk Si and substrate-strained Si devices.

The drain current (I_{ds}) of substrate-strained Si device increases about +5.8% after the application of 0.037% mechanical strain (Fig. 1). The strain level has been measured by Raman spectroscopy and simulated by finite element method.[10] In contrast, the saturation drain current of bulk Si PFET decreases about 3.3%. It is noted that the threshold voltage change is negligible, due to the small biaxial tensile strain.[11] The peak mobility of substrate-strained Si device under the mechanical strain increases about +4.0%, but the peak mobility of bulk Si PFET decreases about 2.1% (Fig. 2). The hole mobility is extracted from split *C-V* technique

[a)]Author to whom correspondence should be addressed; electronic mail: chee@cc.ee.ntu.tw

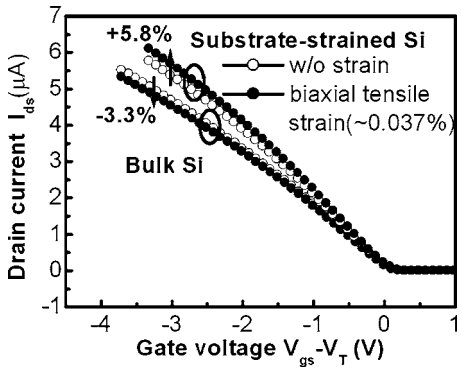

FIG. 1. The drain current of bulk Si devices and substrate-strained Si devices. After strain application, the drain current of the bulk Si devices decreases while the drain current of substrate-strained Si devices increases.

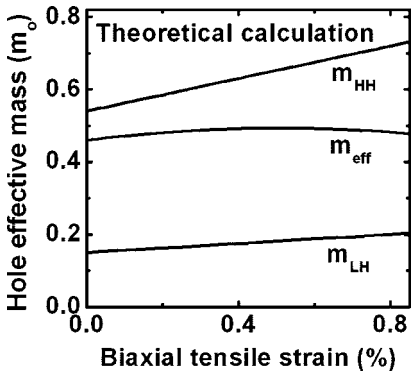

FIG. 3. The hole masses as a function of strain. The effective hole conductive mass (m_{eff}) increases slightly at small tensile strain and then decreases at the large tensile strain.

using the device with the channel length of 100 μm and the channel width of 200 μm. Note that the total strain in the substrate-strained Si PFET under mechanical strain is the sum of the substrate strain (0.64%) and the mechanical strain (0.037%). Due to the channel length (L=100 μm) and thick gate oxide (~30 nm) in our device, the mobility at the high electric field and the influence of quantum-mechanical confinement in the out-of-plane direction are not considered in this work. The peak mobilities of the four curves in Fig. 2 occur at low field (<0.3 MV/cm) where the quantum-mechanical effect can be neglected, and the dominating scattering should be phonon scattering.[1] By solving the Schrodinger equation with the six-band $\mathbf{k}\cdot\mathbf{p}$ method,[12–15] the hole conductive effective mass (m_{eff}) is obtained by the second derivatives of band structure. Figure 3 shows the heavy-hole (m_{HH}) and light-hole (m_{LH}) masses as a function of biaxial tensile strain, and both masses increase monotonically with strain. Since holes are populated in both the light-hole and the heavy-hole bands, the m_{eff} is a population average of heavy holes and light holes using the formula

$$m_{\text{eff}}(\varepsilon) = \frac{m_{(\text{LH})}(\varepsilon)N_{V(\text{LH})}(\varepsilon) + m_{(\text{HH})}(\varepsilon)N_{V(\text{HH})}(\varepsilon)e^{-\Delta E(\varepsilon)/k_BT}}{N_{V(\text{LH})}(\varepsilon) + N_{V(\text{HH})}(\varepsilon)e^{-\Delta E(\varepsilon)/k_BT}}, \tag{1}$$

where $N_V(\varepsilon)$ is the density of state as a function of strain, k_B is the Boltzmann constant, and T is the absolute temperature.

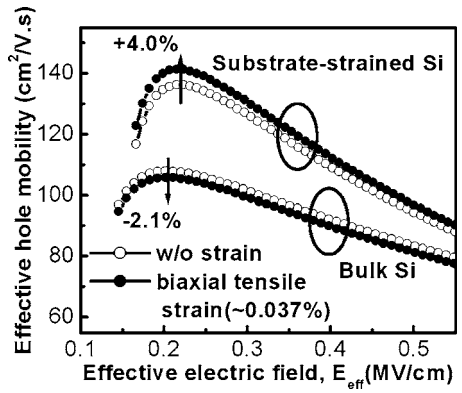

FIG. 2. Effective hole mobility of bulk Si and the substrate-strained Si devices with/without biaxial tensile strain of 0.037%.

The band splitting energy $\Delta E(\varepsilon)$ is given as a function of the strain ε:[16]

$$\Delta E(\varepsilon) = |3b \times (\varepsilon_3 - \varepsilon_1)|, \tag{2}$$

$$\varepsilon_1 = (S_{11} + S_{12}) \times E \times \varepsilon, \tag{3}$$

$$\varepsilon_3 = 2S_{12} \times E \times \varepsilon, \tag{4}$$

where b, E, $S_{11}(S_{12})$, and ε are the band splitting deformation potentials, Young's modulus, the elastic constants, and the biaxial strain, respectively. At small biaxial tensile strain, the conductive effective mass is more heavy-hole-like, since the heavy-hole band has a larger density of state than the light-hole band. The large strain induces upshift of the light-hole band and more holes are occupied in the light-hole band. Therefore, the effective mass under large strain decreases significantly due to the small mass of light hole but increases at small biaxial tensile strain.

The calculation of the momentum relaxation time is complicated due to anisotropy and nonparabolicity of the hole dispersion. Since only the peak mobility is of interest, the phonon scattering including acoustic and optical phonons is taken into account in this letter. The calculation of scattering rate is implemented by the methods of prior work.[17–19]

$$\frac{1}{\tau_{\text{acoust}}(E,\varepsilon)} = \frac{2\pi K_B T_0 \varepsilon_{\text{Si}}^2}{h\rho_{\text{Si}} u_{l,\text{Si}}^2}[D_{\text{HH}}(E - \Delta E(\varepsilon)) + D_{\text{LH}}(E)], \tag{5}$$

$$\frac{1}{\tau_{\text{optical}}(E,\varepsilon)} = \frac{\pi h D_t K_{\text{Si}}^2}{\rho_{\text{Si}} K_B \theta_{\text{Si}}}\{N[D_{\text{HH}}(E - \Delta E(\varepsilon) + K_B\theta_{\text{Si}}) + D_{\text{LH}}(E + K_B\theta_{\text{Si}})] + (N+1)[D_{\text{HH}}(E - \Delta E(\varepsilon) - K_B\theta_{\text{Si}}) + D_{\text{LH}}(E - K_B\theta_{\text{Si}})]\}, \tag{6}$$

$$\frac{1}{\tau_{\text{HH}}(E,\varepsilon)} = \frac{1}{\tau_{\text{HH,acoust}}(E,\varepsilon)} + \frac{1}{\tau_{\text{HH,optical}}(E,\varepsilon)}, \tag{7}$$

$$\frac{1}{\tau_{\text{LH}}(E,\varepsilon)} = \frac{1}{\tau_{\text{LH,acoust}}(E,\varepsilon)} + \frac{1}{\tau_{\text{LH,optical}}(E,\varepsilon)}, \tag{8}$$

$$\langle \tau_{\text{HH}}(\varepsilon) \rangle = \frac{\int_0^\infty \tau_{\text{HH}}(E,\varepsilon)E \times D_{\text{HH}}(E - \Delta E(\varepsilon)) \times f(E)dE}{\int_0^\infty E \times D_{\text{HH}}(E - \Delta E(\varepsilon)) \times f(E)dE}, \tag{9}$$

TABLE I. The numerical value of parameters used in the calculation.

b (eV) (Ref. 23)	E (10^9 Pa) (Ref. 23)	S_{11} (10^{11} Pa) (Ref. 23)	S_{12} (10^{11} Pa) (Ref. 23)	ε (eV) (Ref. 17)	D_tK (10^8 eV/cm) (Ref. 17)	θ (K) (Ref. 17)	ρ (g/cm^3) (Ref. 17)	u_l (10^5 cm/s) (Ref. 17)
−2.35	150	0.77	−0.22	5.12	9.91	735	2.33	9.05

$$\langle \tau_{\mathrm{LH}}(\varepsilon) \rangle = \frac{\int_0^\infty \tau_{\mathrm{LH}}(E,\varepsilon) E \times D_{\mathrm{LH}}(E) \times f(E) dE}{\int_0^\infty E \times D_{\mathrm{LH}}(E) \times f(E) dE}, \tag{10}$$

$$\langle \tau(\varepsilon) \rangle = m_{\mathrm{eff}}(\varepsilon) \frac{n_{\mathrm{HH}}(\varepsilon) \langle \tau_{\mathrm{HH}}(\varepsilon) \rangle}{n(\varepsilon) m_{\mathrm{HH}}(\varepsilon)} + m_{\mathrm{eff}}(\varepsilon) \frac{n_{\mathrm{LH}}(\varepsilon) \langle \tau_{\mathrm{LH}}(\varepsilon) \rangle}{n(\varepsilon) m_{\mathrm{LH}}(\varepsilon)}, \tag{11}$$

$$\frac{\Delta \mu(\varepsilon)}{\mu(\varepsilon)} = \frac{\Delta \langle \tau(\varepsilon) \rangle}{\langle \tau(\varepsilon) \rangle} - \frac{\Delta m_{\mathrm{eff}}(\varepsilon)}{m_{\mathrm{eff}}(\varepsilon)}, \tag{12}$$

where $D(E)$ is the density of state, $f(E)$ is the Fermi-Dirac distribution function, N is the Bose-Einstein distribution, and n is the carrier concentration. The material parameters used in the calculation are given in Table I.

Figure 4 shows that a "large enough" biaxial tensile strain is necessary to enhance the hole mobility. Under the biaxial tensile strain (0.037% used in our experiment), the peak hole mobility degrades, since the splitting of the heavy-holes and light-holes is too small to reduce the scattering rate and the increasing hole effective mass at the small strain is the dominant factor to degrade the mobility. The result that the mobility under small strain is affected mainly by the change of effective mass is also reported in the literature.[19] On the other hand, the mobility enhancement of the substrate-strained Si device under the additional biaxial tensile mechanical strain is observed. The band edge of light-holes now is far above that of heavy-holes under the large total strain, sum of substrate strain and mechanical strain. The scattering rate becomes smaller after the application of mechanical biaxial tensile strain to the substrate-strained Si device and the hole conductive effective mass decreases with small strain at the strain level of 0.64%. This leads to the enhanced hole mobility of substrate-strained Si devices under the biaxial tensile mechanical strain.[20–22] Note that the previous simulation at the intermediate field (~0.3 MV/cm) in Ref. 24 only shows the monotonic increase of mobility under biaxial tensile strain.

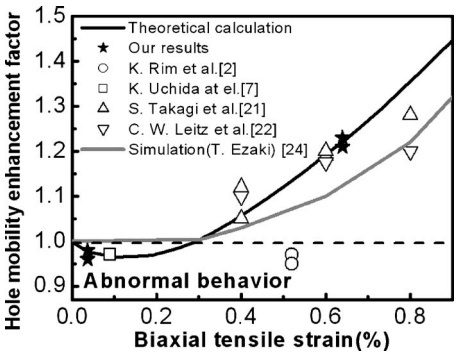

FIG. 4. Hole mobility enhancement factor as a function of biaxial strain. The mobility degradation is observed at small biaxial tensile strain.

In conclusion, the different trends of the hole mobility change for the bulk Si FETs and substrate-strained Si FETs under the biaxial tensile mechanical strain are observed and studied quantitatively. The abnormal hole mobility under small biaxial tensile strain is shown to originate from the effective hole conductive mass, which increases at small strain, then decreases at large strain. The calculation is in a good agreement with experimental data. This investigation will be helpful to find a way of strain technology for the improvement of p-channel MOSFETs.

This work is supported by National Science Council of ROC under Contract Nos. 93-2215-E-002-003 and 93-2215-E-002-017.

[1] J. L. Hoyt, H. M. Nayfeh, S. Eguchi, I. Aberg, G. Xia, T. Drake, E. A. Fitzgerald, and D. A. Antoniadis, Tech. Dig. - Int. Electron Devices Meet. 23 (2002).
[2] K. Rim *et al.*, Symp. VLSI Tech. Dig. 98 (2002).
[3] M. H. Lee *et al.*, Tech. Dig. - Int. Electron Devices Meet. 69 (2003).
[4] C. W. Liu, M. H. Lee, Y. C. Lee, P. S. Chen, C.-Y. Yu, J.-Y. Wei, and S. Maikap, Appl. Phys. Lett. **85**. 4947 (2004).
[5] K. Mistry *et al.*, Symp. VLSI Tech. Dig. 50 (2004).
[6] B. M. Haugerud, M. B. Nayeem, R. Krithivasan, Y. Lu, C. Zhu, J. D. Cressler, R. E. Belford, and A. J. Joseph, Solid-State Electron. (submitted).
[7] K. Uchida, R. Zednik, C.-H. Lu, H. Jagannathan, J. McVittie, P. C. McIntyre, and Y. Nishi, Tech. Dig. - Int. Electron Devices Meet. 229 (2004).
[8] S. Maikap, C. Y. Yu, S. R. Jan, M. H. Lee, and C. W. Liu, IEEE Electron Device Lett. **25**, 40 (2004).
[9] W.-C. Hua, M. H. Lee, P. S. Chen, S. Maikap, C. W. Liu, and K. M. Chen, IEEE Electron Device Lett. **25**, 693 (2004).
[10] M. H. Liao, M.-J. Chen, T. C. Chen, P. L. Wang, and C. W. Liu, Appl. Phys. Lett. **86**, 223502 (2005).
[11] S. E. Thompson, G. Sun, K. Wu, J. Lim, and T. Nishida, Tech. Dig. - Int. Electron Devices Meet. 221 (2004).
[12] H. Hasegawa, Phys. Rev. **129**, 1029 (1963).
[13] G. Dresselhaus, A. F. Kip, and C. Kittel, Phys. Rev. **98**, 368 (1955).
[14] S. L. Chuang, *Physics of Optoelectronic Devices* (Wiley-Interscience, New York, 1995), p. 144.
[15] S. Rodriguez, J. A. L. Villanueva, I. Melchor, and J. E. Carceller, J. Appl. Phys. **86**, 438 (1999).
[16] J. S. Lim, S. E. Thompson, and J. G. Fossum, IEEE Electron Device Lett. **25**, 731 (2004).
[17] F. M. Bufler and B. Meinerzhagen, J. Appl. Phys. **84**, 5597 (1998).
[18] R. Oberhuber, G. Zandler, and P. Vogl, Phys. Rev. B **58**, 9941 (1998).
[19] M. V. Fischetti, Z. Ren, P. M. Solomon, M. Yang, and K. Rim, J. Appl. Phys. **94**, 1079 (2003).
[20] S. Maikap, M. H. Liao, F. Yuan, M. H. Lee, C. F. Huang, S. T. Chang, and C. W. Liu, Tech. Dig. - Int. Electron Devices Meet. 233 (2004).
[21] S. Takagi, Tech. Dig. - Int. Electron Devices Meet. (2003).
[22] C. W. Leitz, M. T. Currie, M. L. Lee, Z.-Y. Cheng, D. A. Antoniadis, and E. A. Fitzgerald, J. Appl. Phys. **92**, 3745 (2002).
[23] In *Properties of Crystalline Silicon*, EMIS Datareviews Series No. 20, edited by R. Hull (INSPEC, London, 1999).
[24] *Simulation of Semiconductor Processes and Devices 2004* (SISPAD 2004), edited by G. Wachutka and G. Schrag (Springer, Vienna, 2004), p. 53.